Meteorol Atmos Phys 83, 67–88 (2003)
DOI 10.1007/s00703-002-0561-y

Meteorology and Atmospheric Physics
Printed in Austria

Institut für Geophysik und Meteorologie, Köln, Germany

Long-term precipitation variability in Morocco and the link to the large-scale circulation in recent and future climates

P. Knippertz, M. Christoph, and **P. Speth**

With 16 Figures

Received July 19, 2001; revised May 31, 2002
Published online: September 23, 2002

Summary

Monthly precipitation data from the Global Historical Climatology Network for 42 stations in Morocco and its vicinity are investigated with respect to baroclinicity, storm track and cyclone activity, moisture transports, North Atlantic Oscillation (NAO) variations, and different circulation types by means of correlation and composite studies. The results are related to a climate change scenario from an ECHAM4/OPYC3 transient greenhouse gas only (GHG) simulation. Precipitation in northwestern Morocco shows a clear link to the baroclinic activity over the North Atlantic during boreal winter (DJF). In large precipitation months the North Atlantic storm track is shifted southward, more westerly and northwesterly circulation situations occur and moisture transports from the Atlantic are enhanced. The occurrence of local cyclones and upper-level troughs is more frequent than in low precipitation months. The negative correlation to the NAO is relatively strong, especially with Gibraltar as a southern pole (-0.71). The northward shift of the storm track and eastward shift of the Azores High predicted by the ECHAM model for increasing GHG concentrations would therefore be associated with decreasing precipitation and potentially serious impacts for the future water supply for parts of Morocco. In the region south of the Atlas mountains, moisture transports from the Atlantic along the southern flank of the Atlas Mountains associated with cyclones west of Morocco and the Iberian Peninsula can be identified as a decisive factor for precipitation. Northeastern Morocco and Northwestern Algeria, however, is rather dominated by the influence of cyclones over the Western Mediterranean that are associated with a strong northwesterly moisture transport. As both regions appear to be less dependent on the North Atlantic storm track and more on local processes, a straight forward interpretation of the large-scale changes predicted by the ECHAM4/OPYC3 cannot be done without the application of down-scaling methods in the future.

1. Introduction

Parts of Morocco and southwestern Europe have suffered from a series of dry years since the late 1970s including the winter of 1999/2000. Hurrell and van Loon (1997) assigned some of the reduction in precipitation to the North Atlantic Oscillation (NAO) extremes in the 1980s and 1990s. Rodó et al (1997) suggested a possible connection between a severe decrease in precipitation in parts of Spain and the strong/very strong warm phases of the El Niño-Southern Oscillation (ENSO). An ENSO influence on precipitation in Northwest Africa was revealed by Nicholson and Kim (1997) and Ward et al (1999). Hulme (1992) investigated gridded precipitation data and found an increase in the relative variability of annual rainfall south of the Atlas Mountains from the period of 1931–60 to 1961–90. It is not clear if this is just part of natural variability or an indication of climate change and whether this change is anthropogenic or not. Undoubtedly semi arid regions – particularly the south and east of Morocco – are confronted with a high year-to-year precipitation variability and are therefore

highly sensitive to climate change (Gleick, 1992; Bullock and Le Houérou, 1996). In addition, most parts of Morocco are mountain areas, which are known to be potentially vulnerable to the impacts of global warming (Beniston and Fox, 1996). An investigation of possible consequences of a climate change for the Moroccan High Atlas for example revealed great impacts for live-stock management, arboriculture and tourism (Parish and Funnell, 1999). Therefore understanding reasons for precipitation variability is a decisive key to manage future problems with water supply.

Morocco is situated at the southern edge of the mid-latitude storm track. Lying within the influence zone of the Atlantic, the Mediterranean and the Sahara, together with very steep orography, a lot of influence factors on precipitation, both local and large-scale, could be considered. Relatively few studies, however, investigate Moroccan precipitation variability and its links to the large-scale atmospheric circulation in particular. Some work was done with respect to the influence of the NAO and ENSO on rainfall in Morocco (Lamb and Peppler, 1987; Lamb et al, 1997; Ward et al, 1999), even the potential for seasonal prediction on the basis of the respective indices was investigated (El Hamly et al, 1998). Besides station data, tree-ring chronologies of cedars from the Rif, the High and the Middle Atlas were used for the identification of spatio-temporal patterns of drought (Chbouki et al, 1995) or a reconstruction of a winter season NAO series (Stockton and Glueck, 1999). Some other mechanisms that were investigated for countries in the vicinity might be relevant for Moroccan precipitation as well. Zorita et al (1992) regarded the influence of large-scale sea surface temperatures (SST) and sea-level pressure (SLP) in the North Atlantic area on winter precipitation on the Iberian Peninsula and found a clear domination of the atmospheric circulation over the oceanic influences. Ulbrich et al (1999) revealed a southward shift of the activity of baroclinic waves and enhanced westerly humidity advection during winters with high precipitation in Portugal and an additional positive effect by local cyclones. The importance of westerly circulation weather types was confirmed by studies of Zhang et al (1997) and Trigo and DaCamara (2000).

This study addresses the observed large and regional scale conditions for winter precipitation in three different regions of Morocco (and parts of Algeria) and possible future changes. The climate of the period 1931–1998 is investigated on a monthly basis by means of correlation and composite studies (Sects. 4–6). Since a large set of different meteorological factors is considered and related to each other, the picture of the mechanisms involved in precipitation generation presented in earlier studies is completed and elaborated. The separate consideration of three precipitation regions allows to demonstrate the differing importance of meteorological influence factors on a small scale. In order to assess possible future changes, the precipitation–circulation relationship found for the observed climate is used to evaluate results from a climate change scenario simulation with the ECHAM4/OPYC3 (Sect. 7). For both parts of the study similar sets of parameters are considered. The large-scale circulation is represented by the phase of the NAO (cf. Rogers, 1984; Jones et al, 1997), the frequency of circulation types (after Jones et al, 1993) and the horizontal distribution of SLP and lower-tropospheric humidity advection. Synoptic activity is represented by the frequency of cyclones at the surface (using identification schemes by Murray and Simmonds, 1991; Haak and Ulbrich, 1996) and by the synoptic-scale variance (see Christoph et al, 1995) and the monthly mean of the 500 hPa geopotential height. Since changes in synoptic activity due to rising greenhouse gas concentrations were found to be connected to large-scale changes in the horizontal temperature distribution (Knippertz et al, 2000), the upper-tropospheric maximum Eady growth rate was considered to monitor changes in baroclinicity. At the beginning of this paper, the data set and the precipitation index used in this study are described (Sects. 2 and 3). Section 8 contains a short summary and some conclusions and remarks.

2. Data

The monthly accumulated precipitation data used in this study are taken from the Global Historical Climatology Network (GHCN) data set and has been provided by the Office of Climatology of the Arizona State University. A description of an earlier version of this data set can be found in Vose et al (1992). We selected 42 stations in

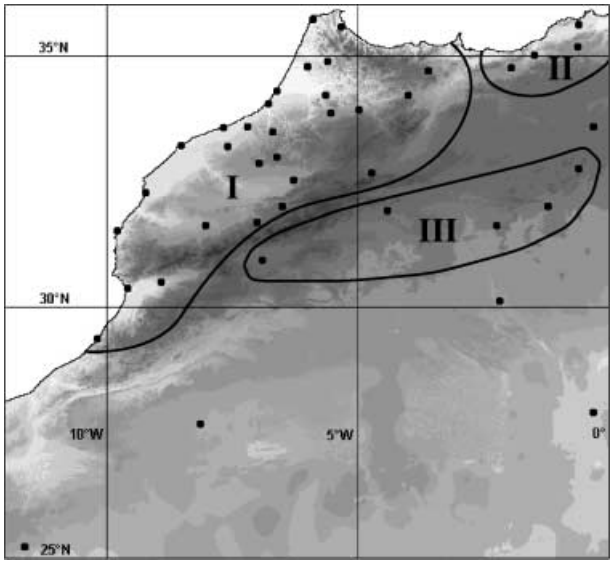

Fig. 1. Region definition for the precipitation index calculation. (I) Atlantic (ATL) region, (II) Mediterranean (MED) region, and (III) the region south of the Atlas (SOA). Black circles indicate the location of the 42 stations considered (see Table 1). The four Saharan stations have not been used for index calculations because of small precipitation amounts, Mecheria because of the short time series available. Shading indicates elevation above sea level

Morocco, Western Algeria and Northern Mauritania (for geographical distribution see Fig. 1, for further information Table 1) with sufficiently long time series. Especially in the semi-arid regions of the area, where many months are entirely dry, strong, but realistic rainfall events might have been eliminated from the data set by the automatic quality control of the GHCN (Russell S. Vose, Office of Climatology of the Arizona State University, pers. comm., 1999). Therefore we checked these removed values on spatial consistency (comparing rainfall amounts to the ones of stations nearby) and meteorological plausibility (considering weather charts of the respective months if available) and re-inserted the months that appeared to be realistic into the data set (less than 1%). Besides, reports from Moroccan stations obtained from the Direction de la Météorologie Nationale (Moroccan weather service) were added to close some gaps in the GHCN data set, especially during the 1980s and 1990s. The investigations are confined to the period 1931–1998, when data coverage is best (Fig. 2a). Only among the Algerian stations in the 1970s larger gaps appear. The solid line in Fig. 2b shows the number of stations with data available for each month of the period considered, that varies between 30 (early 1930s, 1960s, 1970s) and 40 (1940s, 1959s and 1990s).

From the monthly station data annual accumulated rainfall amounts were calculated. As the rainy season in Morocco is the winter half year, these values refer to the time from September to August of the following year. If only one month

Table 1. List of GHCN stations in Morocco, Algeria (*) and Mauritania (**). Latitudes and longitudes to 1/100 of a degree, elevation above sea level in meters. "Period" refers to the first and the last year with data (see Fig. 1)

Nr.	Name	Lat	Lon	Elev	Period
1	Oran/Es Senia*	35.63	−0.60	90	1900–2000
2	Tlemcen/Zenata*	35.02	−1.47	247	1922–2000
3	Sidi-Bel-Abbas*	35.18	−0.63	486	1901–2000
4	Mecheria*	33.60	−0.30	1175	1938–2000
5	Ain Sefra*	32.77	−0.60	1058	1901–2000
6	Beni Ounif*	32.00	−1.20	810	1905–1961
7	Bechar*	31.62	−2.23	806	1906–2000
8	Beni-Abbes*	30.13	−2.17	498	1921–2000
9	Adrar*	27.90	−0.30	264	1906–2000
10	Tindouf Ville*	27.67	−8.13	402	1935–2000
11	Bir Moghrein**	25.23	−11.62	359	1942–1999
12	Tangiers	35.73	−5.90	14	1900–2000
13	Souk Larbat	34.80	−6.00	60	1917–1998
14	Ouezzene	34.90	−5.60	170	1931–1995
15	Aknoul	34.70	−3.60	1200	1932–1998
16	Oujda	34.78	−1.93	468	1931–2000
17	Kenitra	34.30	−6.60	12	1926–2000
18	Taza	34.22	−4.00	510	1923–2000
19	Rabat	34.05	−6.77	84	1930–2000
20	Rommani	33.50	−6.70	300	1918–1997
21	Sidi Kacem	34.23	−5.65	90	1914–1996
22	Fes	33.93	−4.98	579	1914–2000
23	Midelt	32.68	−4.73	1515	1931–2000
24	Ben Slimane	33.60	−7.20	188	1913–1999
25	Meknes	33.88	−5.53	549	1931–2000
26	Casablanca	33.57	−7.67	58	1902–2000
27	Settat	33.20	−7.60	368	1909–1998
28	El Jadida	33.23	−8.52	28	1931–2000
29	Khouribga	32.87	−6.97	785	1925–2000
30	Oued Zem	33.00	−6.60	827	1925–1996
31	Safi	32.28	−9.23	45	1900–2000
32	Kasba-Tadla	32.53	−6.28	507	1915–2000
33	Azilal	32.00	−6.50	1350	1917–1993
34	Er Rachidia	31.93	−4.40	1045	1936–2000
35	Mogador	31.52	−9.78	8	1900–2000
36	Marrakech	31.62	−8.03	466	1900–2000
37	Agadir	30.38	−9.57	19	1921–2000
38	Taroudant	30.50	−8.90	265	1931–2000
39	Ouarzazate	30.93	−6.90	1136	1931–2000
40	Demnate	31.70	−7.00	960	1927–2000
41	Sidi Ifni	29.37	−10.18	66	1951–2000
42	Tetouan	35.58	−5.33	10	1918–2000

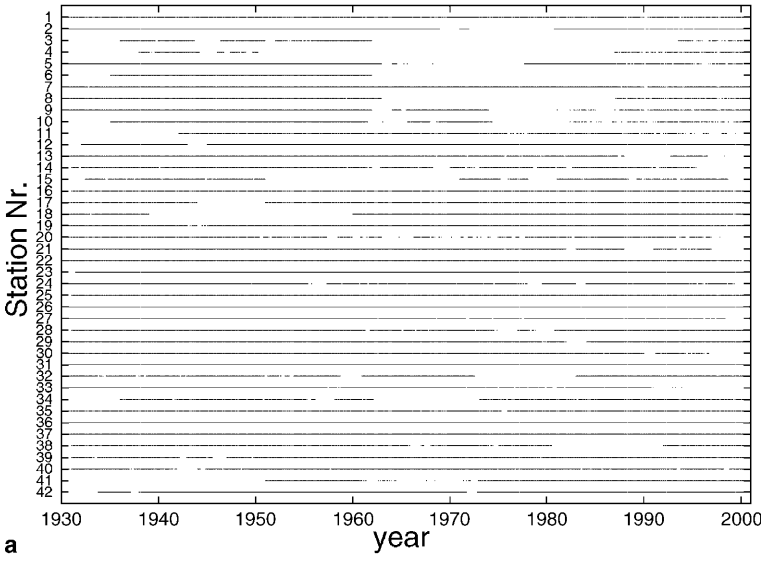

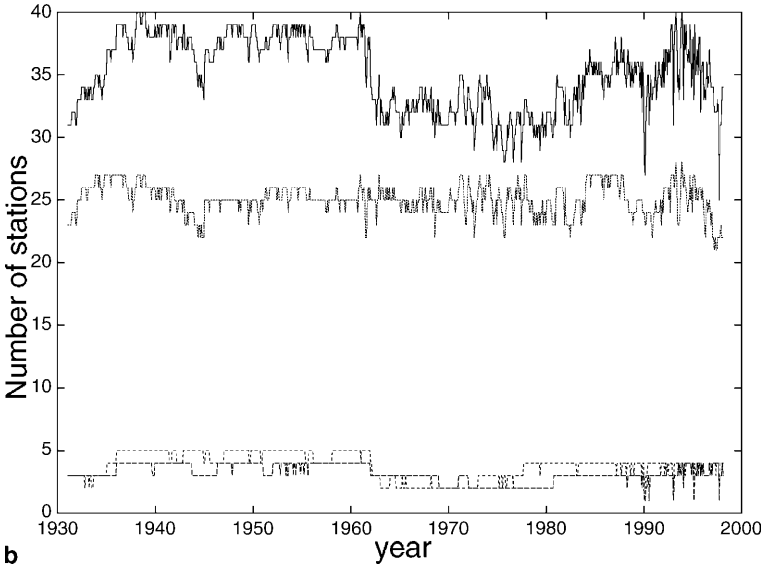

Fig. 2a. Data availability for the 42 GHCN precipitation stations in Morocco, Algeria and Mauritania for the period from 1930 to 2000 (for station locations see Fig. 1). The station numbers correspond to the ones in Table 1. Every dot on the diagram represents one month with data; **b** Number of stations available for each month: All stations (solid line), ATL (dotted line), MED (long dashes) and SOA region (short dashes); for definitions of the regions, see Fig. 1

within a year has no data, it was replaced by the long-term monthly mean calculated from all data available for the respective month. The monthly and yearly accumulated precipitation data are used to determine the mean, standard deviation, minimum and maximum and mean annual cycles, which agree with climatologies like in Griffiths (1972). Detailed orographic influences on precipitation such as a maximum over the mountains of Morocco, however, are not resolved, because of the lack of stations in mountainous areas. In order to give an example of the use of this data and to demonstrate the large relative year-to-year variability, the coefficient of precipitation variation (see e.g., Hulme, 1992) is shown in Fig. 3. Values between around 25% close to the Atlantic coast and over 100% in the Sahara reveal the rather low reliability of rainfall for the whole area.

For the representation of the large-scale circulation in Sects. 5 and 6 the NCEP (National Centers for Environmental Prediction) re-analysis, that are available in 2.5° horizontal resolution for the period from 1958–1998, was used. Except of humidity, that is more strongly influenced by the analysis model, basic meteorological quantities (temperature, SLP, geopotential and wind) are used for this investigation, that are considered to be most reliable and closest to observations (Kalnay et al, 1996). The NAO indices and COADS (Comprehensive Ocean-Atmosphere Data Set) pressure data (Sect. 4) and the data

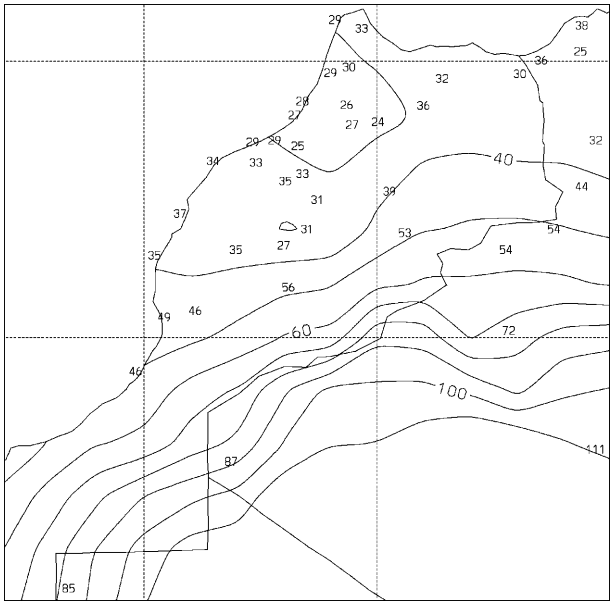

Fig. 3. Relative annual precipitation variability (the coefficient of variation, i.e. standard deviation standardized by the mean in percent) for the 42 stations from Table 1. Contour interval is 10%

from the ECHAM4/OPYC3 greenhouse gas only scenario (Sect. 7) will be presented in the respective sections. We took only winter months (December to February, DJF) into account, since most stations show a precipitation maximum during this time of the year.

The significance of differences between two ensembles (the positive and negative composite in Sect. 6 and the climate signal in Sect. 7) is calculated with a simple two-sided *t*-test applied to the variance of the month-to-month and the winter-to-winter variability, respectively. An exception is made for cyclone frequency. Since this quantity is not normally distributed, differences are tested with a χ^2-test (for details see Sect. 6). For the significance of correlations an *F*-test was employed (Taubenheim, 1969). Since the monthly precipitation values for winter show absolute values of one-month-lag auto-correlations below 0.15 for all stations considered, no reduction of the degrees of freedom had to be applied. Significant values are shaded in the respective figures.

3. Precipitation index

In principle, complete and homogeneous time series are desirable for all kinds of climatological investigations. In many cases, it makes sense to confine an observational data set to the stations and time period, where this condition is satisfied. Such an approach applied to our data set would reduce the available information to few stations (see Sect. 2). We therefore decided to deal with the problem of varying data coverage by calculating precipitation indices that are representative for the precipitation in a certain area (e.g., Katz and Glantz, 1986). This is a reasonable approach for the present study, since the mostly large-scale nature of winter precipitation in Morocco leads to a spatial coherency of monthly accumulated rainfall. By combining information from different stations an complete index time series can be derived, that is of greater use than partly incomplete time series from single stations.

Concerning the actual computation of the precipitation index, a common way to deal with the problem of weighting stations with significantly different amounts of rainfall is to divide by the respective standard deviation (Katz and Glantz, 1986; Nicholson, 1986). Since many stations, in particular semi-arid ones, have non-Gaussian distributions, when monthly precipitation is considered (cf. Nicholson, 1986), the computation of the index is done on the basis of quintiles basically following the approach in the Monthly Climatic Data for the World published by the National Climatic Data Center (NCDC). Each value (monthly or annual) is assigned to one number from 1 to 5 depending on which 20% portion of the distribution it belongs to (1 for the 20% lowest values, 2 for the lower 20–40% etc.). The precipitation index is defined as the mean of these quintiles averaged over all stations available within one region at a given time. Precipitation index anomalies can then be calculated by subtracting the median value of 3 giving a range of index values from -2 to 2. A similar approach (but with percentiles instead of quintiles) was used by Rasmusson and Carpenter (1983) for precipitation in India.

We distinguish 3 regions in the area of interest (Fig. 1), which were identified by cross-correlating monthly precipitation at the 42 stations: The northern and western parts of Morocco (called ‘‘Atlantic region (ATL)’’ hereafter), the Northeast of Morocco and the Northwest of Algeria close to the Mediterranean coast (‘‘Mediterranean region (MED)’’) and the Moroccan and Algerian stations south of the Atlas mountains (‘‘Atlas region

(SOA)''). The 4 Moroccan and Algerian stations in the Sahara are not considered because of their small rainfall amounts. Mecheria in Western Algeria (see Table 1 and Fig. 1) has relatively few data available and does not show large correlations to either the stations of the SOA nor the MED region and was therefore not considered either. The average pairwise correlation between stations within one region for DJF (ATL 0.74, MED 0.75, SOA 0.42) give evidence that there is a good coherency of the temporal behaviour of precipitation within one region. The fact that – except of the SOA region – these values are larger than the correlation between the different indices ($r(ATL/MED) = 0.43$, $r(ATL/SOA) = 0.47$, $r(MED/SOA) = 0.26$) further reveals that the choice of regions is reasonable. The differences in rainfall behaviour between the three regions are presumably partly due to the orography, because the regions are separated from each other by the major mountain chains of the area (the High, Middle, Tell and Sahara Atlas and the Rif). The region definition corresponds to the one determined by Ward et al (1999) using rotated EOFs (empirical orthogonal functions) except from a subdivision of the ATL region into three parts. We tested this approach, but as the composite and correlation studies (see Sects. 4–6) yielded very similar results for the three ''Atlantic regions'', this subdivision does not appear to be more advantageous for our investigations. Considering the maximum number of stations within one region, the percentage of total variance that the index explains is 81% for the MED, 75% for the ATL and 53% for the SOA region for DJF (according to the formula given by Katz and Glantz, 1986, p. 766). For a good reliability of the index for the respective region, small variations of data coverage are essential. The number of station reports per region available for a given month (Fig. 2b) reveals that variations are within an acceptable range for the presented data set (between 2 and 4 or 5 for MED and SOA and around 25 for ATL).

The temporal behavior of the precipitation index on an annual basis is shown in Fig. 4 displaying considerable interannual and decadal variability. In the MED region a pronounced decrease of precipitation since the 1970s is visible, whereas ATL region precipitation is low from the late 1970s to the early 1990s, but reveals some wet years during the late 1990s; SOA region precipitation is above average during most of this period after the mid 1980s. Chbouki et al (1995) identified drought periods from tree-ring chronologies in the Rif, the Middle and High Atlas and found some agreement to our results: a rather wet period 1950–1970 (all three regions) and relatively dry periods during 1925–1950 (SOA) and the 1970s (SOA and ATL). A collection of annual precipitation time series from stations in the Drâa catchment (within the SOA region) from Youbi (1990) shows a behavior similar to the SOA

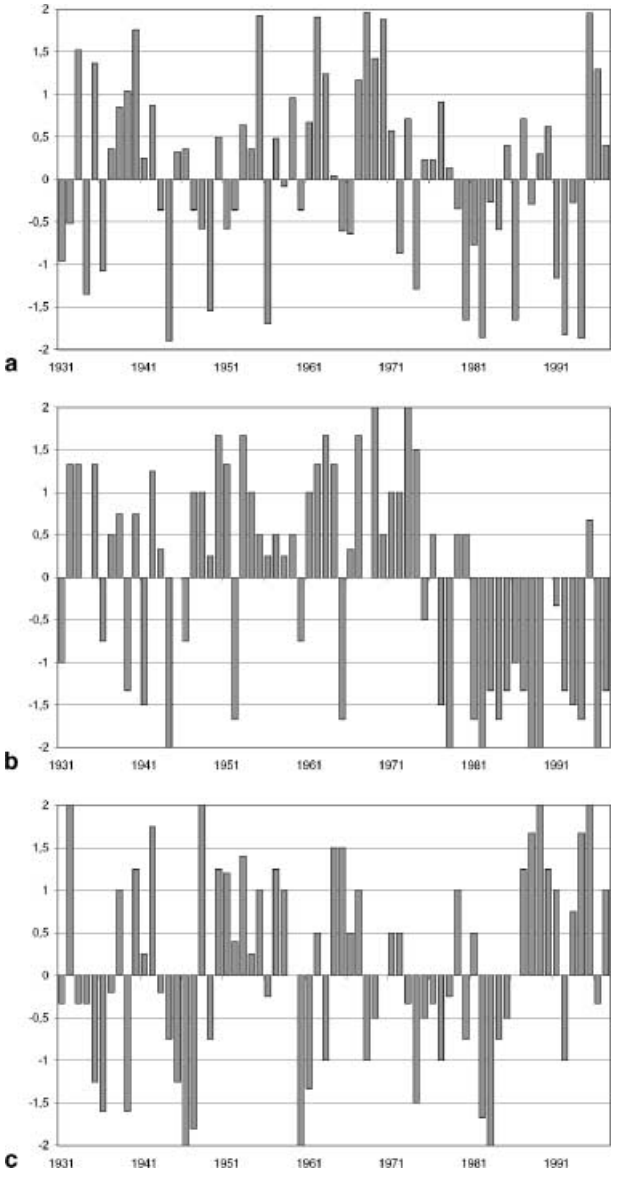

Fig. 4. Time series of annual (September to August) precipitation index anomalies (see text for index definition). Numbers on the x-axis refer to the year of the September; **a** ATL, **b** MED, and **c** SOA region (for definitions of the regions, see Fig. 1)

index. The years from 1981 to 1994 were particularly dry in southwestern Europe and northern Morocco compared to 1951–1980 (Hurrell and van Loon, 1997). This is clearly visible in the MED region index series and less distinct for the ATL region. It is striking that the years, when two strong ENSO warm phases occurred (1982/83 and 1992/93), have been relatively dry in all three regions agreeing with findings for parts of Spain (Rodó et al, 1997), whereas the 1997/98 El Niño has been dry only in the MED region.

4. The influence of the North Atlantic Oscillation

Several studies have investigated or used the influence of the North Atlantic Oscillation (NAO) on Moroccan precipitation variability. Lamb et al (1997) and Ward et al (1999) defined precipitation indices for different regions in Morocco and calculated correlations on a seasonal and a monthly basis with the NAO index derived from the normalized pressure difference between the Azores and Iceland. They found large negative correlations (up to -0.6) with the precipitation at stations in northern and western Morocco and a decrease towards the south and the east of the country. Largest negative values occur during January and February. Because of the relatively large intraseasonal variability and the resulting little persistency of the NAO, El Hamly et al (1998) used an EOF analysis of the July to April monthly evolution of the NAO aiming at a seasonal prediction for Moroccan precipitation. The strong relationship between seasonal precipitation amounts and biomass production induced Stockton and Glueck (1999) to use tree ring data from cedars in the Middle and High Atlas Mountains for a 550 year reconstructing of a winter season NAO series. A strong influence of the NAO on winter precipitation was also found for the vicinity of Morocco like the Iberian Peninsula (Zorita et al, 1992; Rodó et al, 1997; Ulbrich et al, 1999) or the Canary Islands (García Herrera et al, 2001).

In this study, the sensitivity of the relation to the choice of the NAO centres shall be investigated comparing two different NAO indices (standardized pressure difference Azores-Iceland (NAO-A, cf. Rogers, 1984) and Gibraltar-Iceland (NAO-G, Jones et al, 1997)). Table 2 shows correlations on a monthly basis for DJF, when the NAO is strongest and reveals relatively stable centres (Portis et al, 2001). Monthly correlations were preferred to seasonal, since the NAO has a large intraseasonal variability (month-to-month auto correlations below 0.2 in winter). The negative correlations indicate reduced precipitation, when pressure is lower than normal in the subpolar and higher than normal in the subtropics (positive phase of the NAO). The use of different southern poles of the NAO leads to considerable differences in the strength of the relation (see Table 2). The NAO-G index explains 50% (correlation $r = -0.71$) of the rainfall variance in the ATL region. In some months at some stations 60% (e.g., Tetuan (35.6° N, 5.3° W) in December) explained variance is reached. Values for the SOA ($r = -0.31$) and the MED ($r = -0.25$) region are substantially lower. With less than 10% explained variance, the NAO has obviously little influence on precipitation in these regions. In contrast to that, the NAO-A index accounts only for 24% ($r = -0.49$) of the rainfall variance in the ATL and nearly no variance at all in the other regions.

Table 2. Correlation of monthly precipitation indices with two different NAO indices (NAO-G = NAO index Gibraltar-Iceland, NAO-A = NAO index Azores-Iceland) and station pressure (Gibraltar, Ponta Delgada, Azores and Iceland) for winter (DJF) 1931–1998. Stars indicate significance on the 95% (*) and the 99% (**) level, respectively

	NAO-G	NAO-A	P_{Gib}	P_{Azo}	P_{Ice}
ATL	-0.71^{**}	-0.49^{**}	-0.81^{**}	-0.42^{**}	0.46^{**}
MED	-0.25^{**}	-0.04	-0.31^{**}	0.09	0.14
SOA	-0.31^{**}	-0.14	-0.39^{**}	-0.08	0.18^{*}

From the comparison of the two NAO indices commonly used in literature the question arises, if we can identify other large-scale pressure patterns that explain more precipitation variability than the dominant NAO. We therefore correlated SLP over the whole North Atlantic and Mediterranean (from COADS in 2° resolution) with the precipitation indices from Sect. 3 for winter (DJF) 1931–1996 (Fig. 5). For the MED region no clear pressure pattern evolves except from slightly reduced pressure over the Western Mediterranean. Although precipitation over the SOA region seems to be connected to a northsouth pattern over the Eastern North Atlantic, centres

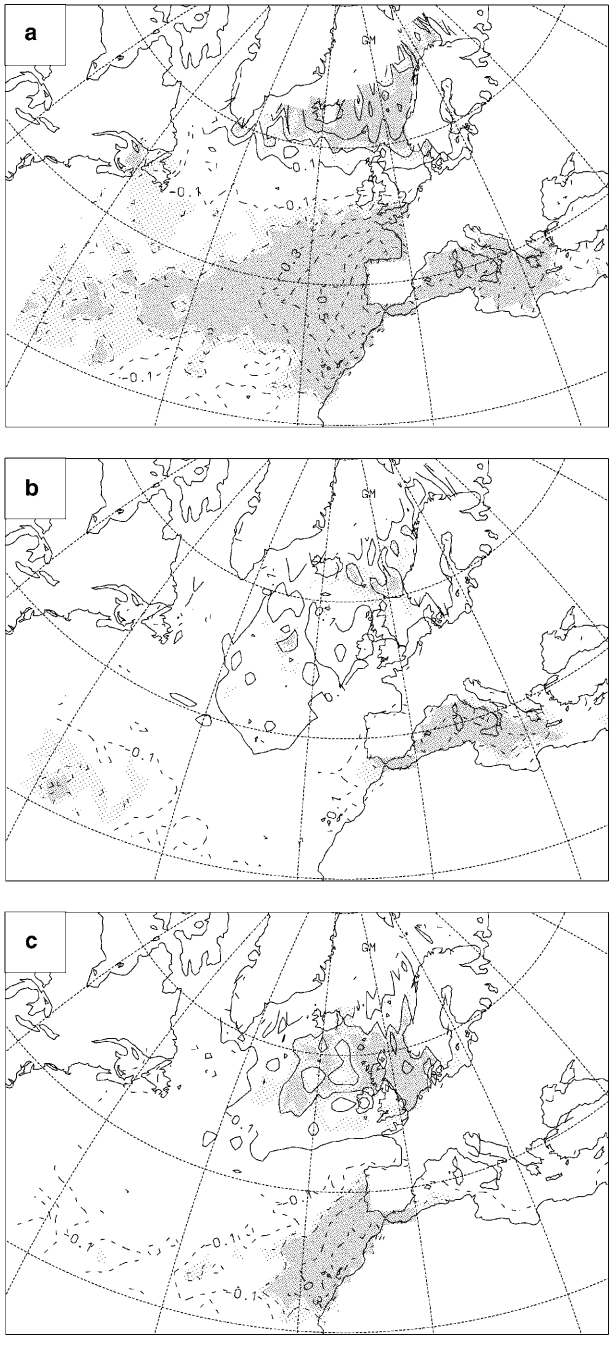

Fig. 5. Correlation of monthly precipitation indices with pressure over the North Atlantic and the Mediterranean for winter (DJF) 1931–1997. Pressure data was taken from COADS (Comprehensive Ocean-Atmosphere Data Set): **a** ATL, **b** MED, and **c** SOA region (for definitions of the regions, see Fig. 1). Contour interval is 0.1. Light and dark shading indicates statistical significance at the 95% and 99% level, respectively

are located far to the south compared to the common NAO centres and correlations are relatively small. In contrast to that, the ATL region shows a NAO like pattern with a clear southern centre southwest of the Iberian Peninsula (correlations up to -0.75) and a band of weaker positive correlations between Southern Greenland and Scandinavia, that resembles a somewhat weaker and southward shifted version of the "optimal" NAO centres found for precipitation in Portugal by Ulbrich et al (1999). The fact that correlations to the southwest of the Iberian Peninsula ($r = -0.81$ at Gibraltar, see Table 2) are substantially higher than anywhere else ($r = -0.42$ on the Azores, $r = 0.46$ on Iceland, see Table 2) suggest that the effect of the NAO on Moroccan precipitation is to a considerable extent a regional rather than a teleconnection effect, since high pressure west of the Iberian Peninsula can most effectively block off synoptic disturbances from the Moroccan Atlantic coast.

5. Circulation weather types

A way to objectively characterize synoptic situations is the approach of circulation weather types (CWTs). 6 hourly SLP data at 16 grid points centred at 35° N and 5° W (see Fig. 6) from the NCEP re-analysis have been used to assign each date to either a rotational (cyclonic (cyc), anticyclonic (ant)), a directional (north (N), northeast (NE), east (E) etc.) or a mixed (half rotational, half directional) circulation type (cf. Jones et al, 1993). The assignment is done on the basis of the strength of the directional flow and the vorticity over the area. The same method was used by Trigo and DaCamara (2000) for an investigation of precipitation variability in Portugal. The SLP patterns obtained by our analysis for each circulation type (not shown) have great similarities to

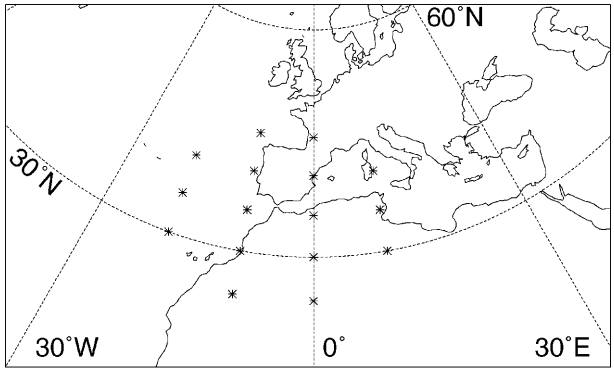

Fig. 6. Location of the 16 grid points used for the calculation of the circulation weather types (after Jones et al, 1993). The grid is centred at 35° N and 5° W

Table 3. Relative frequency (in %) of circulation weather types (after Jones et al, 1993) for winter (DJF) for the grid point 35° N and 5° W. NCEP re-analysis 1958/59–1997/98 (Reana) and two 50 year periods from the beginning (Ctrl) and the end (Scen) of the 240 year transient greenhouse gas simulation with the ECHAM4/OPYC3

	cyc	ant	NE	E	SE	S	SW	W	NW	N
Reana	8.4	41.7	5.9	8.6	8.7	3.2	4.7	6.4	6.5	5.9
Ctrl	4.2	43.1	6.1	10.3	13.5	4.1	4.1	4.5	4.5	5.5
Scen	3.7	40.7	5.5	13.0	20.7	4.8	2.5	2.3	3.0	3.8
Reana-Ctrl	+4.2	−1.4	−0.2	−1.7	−4.8	−0.9	+0.6	+1.9	+2.0	+0.4
Scen-Ctrl	−0.5	−2.4	−0.6	+2.7	+7.2	+0.7	−1.6	−2.2	−1.5	−1.7

the ones for Portugal, but are shifted southward by about 5°. Table 3 shows that Morocco is dominated by anticyclonic situations (41.7%) during winter (DJF). Easterly situations (SE, E, NE), that occur when the center of the subtropical high is located north of Morocco, are also frequent (23.2%). Southerly (S) and southwesterly (SW) circulation types occur least. Correlations between the monthly frequency of each circulation type with the precipitation indices from Sect. 3 (Fig. 7) reveal – not surprisingly – an over all positive influence of cyclonic situations and a negative influence of anticyclonic situations on Moroccan precipitation. The influence of cyclonic circulation types is particularly strong for the SOA region probably due to the westerly humidity advection at the southern flank of cyclones located near 35° N and 5° W (the center of the grid used for the CWT analysis). This relation will be investigated in Sect. 6 (see Fig. 13). In the SOA region the negative influence of anticyclonic CWTs, when dry continental air is advected to the region, is also very strong. Regarding the directional circulation types, westerly situations are found to be favourable, easterly to be unfavorable for precipitation in the ATL region. These only occur, when the Azores High is weak or in a relatively western position, explaining the high negative correlation

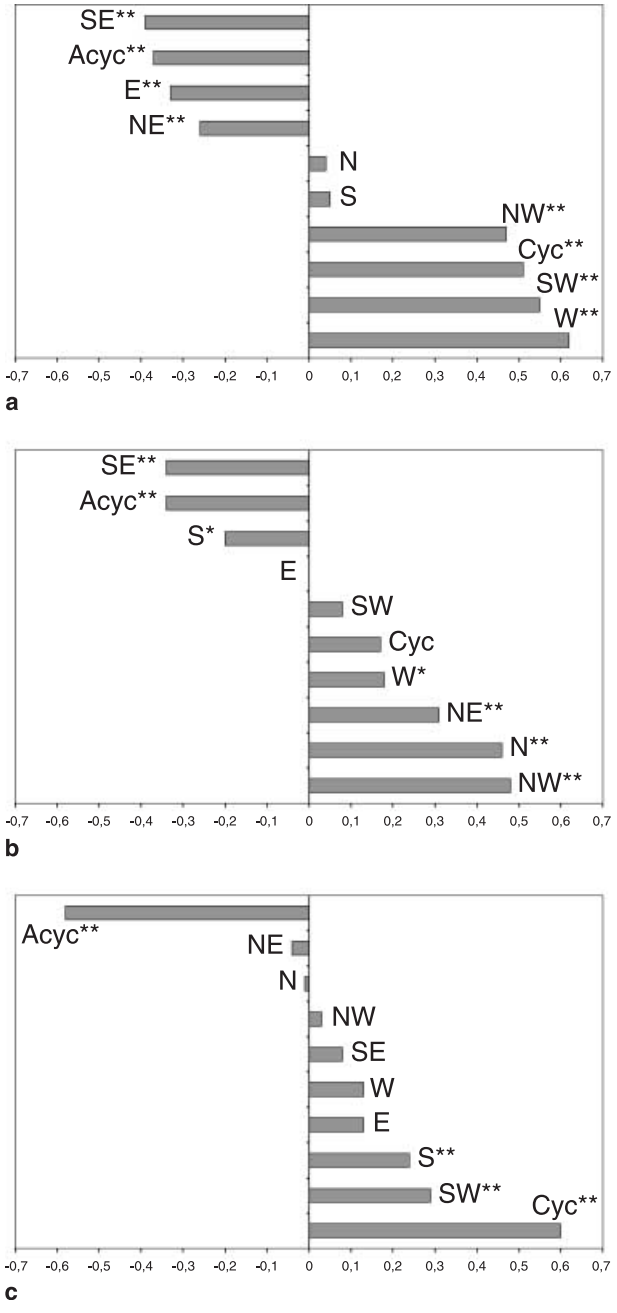

Fig. 7. Correlation of monthly precipitation indices with the frequency of circulation weather types (after Jones et al, 1993, calculated from NCEP re-analysis SLP) for winter (DJF) 1958–1997. Stars indicate significance at the 95% (*) and the 99% (**) level, respectively; **a** ATL, **b** MED, and **c** SOA region (for definitions of the regions, see Fig. 1)

to the NAO index for this region. These results are in agreement with findings for Portugal, where westerly, southwesterly and cyclonic CWTs were found to account for about two thirds of winter precipitation (Trigo and DaCamara, 2000). Similar results were obtained by Zhang et al (1997) with a different method. In the MED region northerly CWTs appear to have the strongest positive influence on precipitation revealing that here (as well as in the ATL region) air flow from the sea nearby plays an important role for rainfall generation. For the SOA region, however, precipitation events are connected with southerly and southwesterly situations. Especially during southerly situations the air flow in low levels is directed against the southern slope of the High Atlas indicating that orographic lifting might play some role in precipitation generation.

6. Composite studies

By looking at differences between means over months with large and small precipitation, the influence of various parameters of the large-scale circulation on Moroccan precipitation can be identified. Emphasis is put on the synoptic and baroclinic activity over the North Atlantic and the Mediterranean. A similar approach was used by Ulbrich et al (1999) for Portugal. We used the monthly precipitation index from Sect. 3 to define composites. Months with an average quintile value below 2 (above 4) were assigned to the negative (positive) composite. The months within the time period of the NCEP re-analysis that fulfil this criterion for the three regions are listed in Table 4. The composites consist of between 26 and 35 months (corresponding to 22% to 29% of the 120 winter months considered) except of the positive composite for the MED region with only 18 months. This is a consequence of the dry 1980s and 1990s in this region, when very few months with large precipitation occurred (see Sect. 3). The underlines in Table 4 reveal that many months were particularly wet or dry in two or even three regions, but there is also a considerable number that belongs to just one composite. In the following, differences between means over all months belonging to the positive and negative composites (Table 4) are presented for several meteorological quantities.

Table 4. Winter (DJF) months from the period 1958/59–1997/98 that were assigned to the positive (precipitation index greater than 4) and the negative (precipitation index smaller than 2) composite for the ATL, the MED and the SOA region (for definitions of the regions see Fig. 1). Underlined months are common to composites of two, double underlined months to the composites of all three regions

ATL		MED		SOA	
pos.	neg.	pos.	neg.	pos.	neg.
195812	196102	195902	195901	195812	195912
196001	196201	196012	196102	195902	196002
196012	196202	196101	196112	196001	196102
196301	196401	196202	196201	196301	196512
196302	196601	196312	196601	196302	196601
196312	196612	196412	196602	196401	196602
196412	196701	196712	196612	196412	196612
196802	196801	196812	196801	196501	196701
196902	197002	196902	197002	196502	197401
197001	197102	197101	197102	196702	197702
197012	197401	197302	197401	196901	197912
197101	197412	197312	197412	196902	198112
197312	197912	197402	197501	197012	198212
197612	198012	197701	197512	197512	198301
197701	198101	197902	197712	197701	198312
197802	198301	198012	197802	197901	198401
197812	198401	199302	197901	198001	198412
197901	198402	199601	198112	198002	198612
197902	198412		198201	198201	198812
198302	198612		198301	198501	199101
198501	198812		198412	198512	199201
198602	199002		198502	198802	199412
198701	199101		198812	198912	199501
198702	199112		198901	199012	199502
198801	199201		199002	199102	199702
198912	199212		199112	199212	199712
199012	199302		199201	199302	
199102	199312		199202	199401	
199402	199412		199212	199601	
199512	199501		199301	199602	
199601	199702		199312	199612	
199612			199412	199701	
199701			199501	199802	
199712			199702		
			199801		

Surface cyclone activity and upper air storm track are related to baroclinic instability, which can be quantified in terms of the maximum Eady growth rate (see Lindzen and Farrell, 1980). It is defined as $\sigma_{BI} = 0.31(f/N)|\delta \mathbf{v}/\delta z|$ where f is the Coriolis parameter, N is the static stability expressed by the Brunt-Väisälä frequency, z is the vertical coordinate and $\mathbf{v}$ is the horizontal wind vector. Representing a characteristic of the atmosphere's basic state, this quantity was not

calculated from daily, but from monthly means of temperature, geopotential height and wind both for the lower (850 hPa to 700 hPa) and the upper troposphere (500 hPa to 300 hPa). Winter mean lower tropospheric baroclinicity (not shown) reveals a distinct maximum off the east coast of North America and a zone of relatively high baroclinicity stretching over the Atlantic into Northern Europe (cf. Hoskins and Valdes, 1990). The upper tropospheric maximum of the Eady parameter (not shown) has a more southwesterly location than its lower tropospheric counterpart. The upper-tropospheric baroclinicity composite differences for the ATL region (Fig. 8) show two dipole-like patterns east and west of the Greenwich Meridian. The latter, representing a clear southward shift of baroclinicity stretching over the whole North Atlantic in months with high precipitation, indicates a southward displacement of the polar front providing good conditions for cyclones to take relatively southern tracks over the Atlantic. This part of the anomaly pattern is hardly visible for the SOA region and not all for the MED region. In contrast to that, the pattern east of the Greenwich Meridian, consisting of a negative pole over Central Europe and a tongue of positive values between Tunisia and Western Turkey, can be clearly identified for all three regions. Since this signal is located downstream of the regions of interest, an interpretation in the sense of a baroclinicity-storm track interaction is quite improbable. Figure 9 shows the composite differences for the 500 hPa geopotential height. Although the exact position of the minima varies between the three regions, precipitation over all Morocco appears to be clearly linked to upper-level troughs close to the Iberian Peninsula. These troughs transport cool maritime air southward leading to a destabilization of the atmosphere and sometimes to local cyclogenesis. Ahead of these troughs relatively warm continental air is transported northward meeting cooler continental air from Eastern Europe over the Mediterranean leading to the zones of enhanced baroclinicity from Fig. 8, whose positions agree quite well with the areas of high geopotential gradients downstream of the troughs. Therefore this part of the baroclinicity anomaly pattern is likely to be rather a consequence of precipitation situations than their actual cause. These results correspond with calculations for the lower troposphere (not shown).

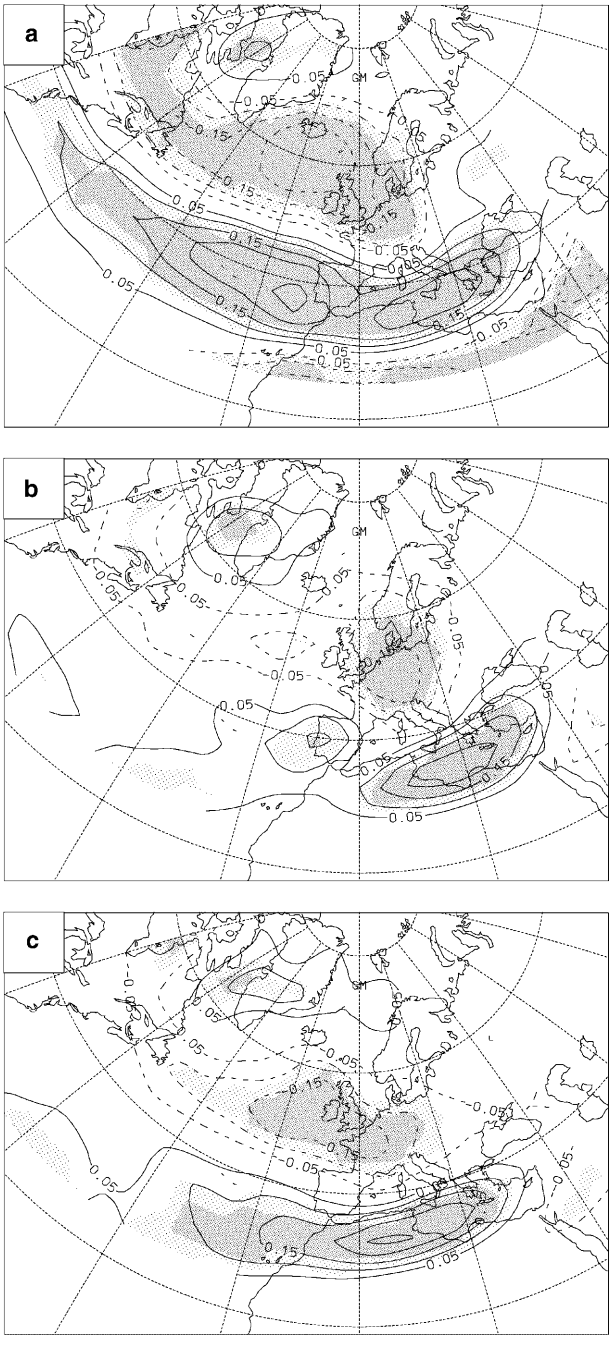

Fig. 8. Composite differences (wet minus dry) for upper-tropospheric (300 hPa to 500 hPa) baroclinicity (measured by the maximum Eady growth rate, see text for definition) for winter (DJF). Contour interval is 0.05 days $^{-1}$. Light and dark shading indicates statistical significance at the 95% and 99% level, respectively; **a** ATL, **b** MED, and **c** SOA region (for definitions of the regions see Fig. 1)

A good indicator for synoptic activity of the mid-latitudes is the upper air storm track activity (here computed from twice daily (00 and 12 UTC) 2.5 to 8 day bandpass filtered 500 hPa

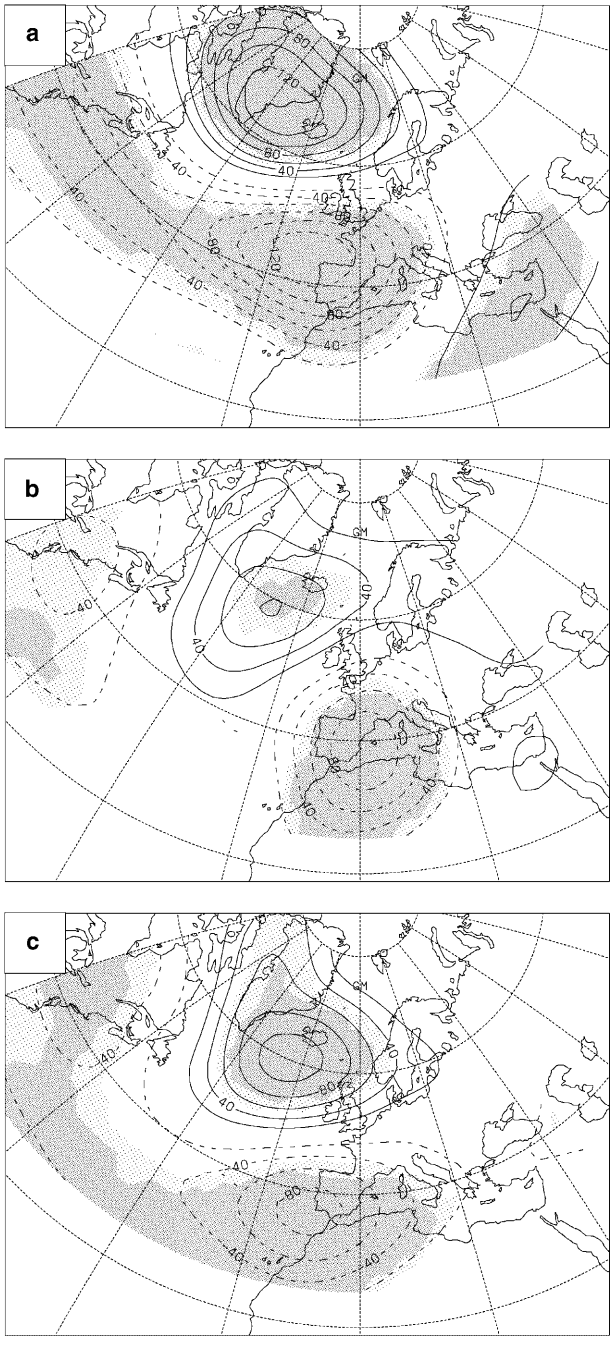

Fig. 9. Same as Fig. 8, but for geopotential height at 500 hPa. Contour interval is 20 gpm

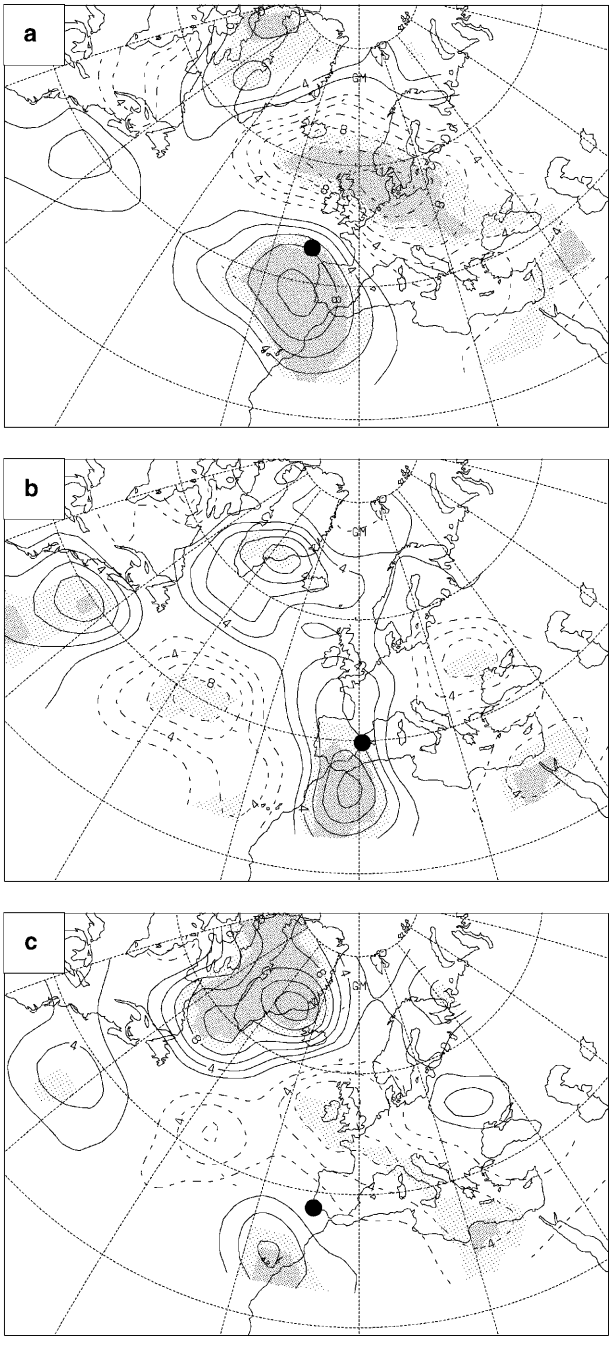

Fig. 10. Same as Fig. 8, but for storm track activity (measured by the 2.5 to 8 day bandpass filtered 500 hPa geopotential height standard deviation as in Christoph et al, 1995). Contour interval is 2 gpm. Black dots represent the minima of geopotential height at 500 hPa from Fig. 9

geopotential height standard deviation as in Christoph et al, 1995). For the ATL region (Fig. 10a) a shift of the eastern end of the North Atlantic storm track activity with high values southwest of the Iberian Peninsula and low values over the North Sea seems to be characteristic for high precipitation months. The southward shift corresponds to the signal in baroclinicity. Since regions of main synoptic activity are usually located downstream of the regions of high baroclinicity, the location of the strongest anomalies is in agreement with the linear theory of baroclinic waves (Charney, 1947; Eady, 1949). For the MED region (Fig. 10b) significant positive storm track anomalies are restricted to areas

close to the region itself. The negative values found over the central northern Atlantic indicate, that precipitation in this region depends more on local activity than on a displacement of the whole storm track like in the ATL region. The anomaly plot for the SOA region (Fig. 10c) shows a tripole-like pattern with weak positive values nearby over the Canary Islands, higher positive values close to Greenland and a zone of negative differences in between. This pattern suggests that a splitting of the storm track into a southern and a northern branch is typical of situations when precipitation in the SOA region is high. Although the storm track anomalies over the Canary Islands are small, they correspond to a relative change of 25% compared to the winter mean (according to Knippertz et al, 2000) at this very southern edge of the storm track. Note that for all three regions the strongest anomalies in storm track activity are located south or southwest of the troughs identified in Fig. 9 as indicated by the black dots in Fig. 10.

Another important factor for precipitation is the frequency and intensity of cyclones. For the identification of cyclone cores a numerical scheme by Murray and Simmonds (1991) on the basis of twice daily (00 and 12 UTC) SLP data was used. After their identification cyclones were counted in 5° lat × 10° lon grid boxes. Since no tracking was applied, it is possible that a cyclone is counted several times depending on the length of its presence in one grid box. The significance of the composite differences is determined with a χ^2-test, but results from this test might be somewhat optimistic, because one event (the occurrence of a cyclone in a grid box) might be not completely independent from another event (if one cyclone is counted several times in the same grid box). Since a cyclone that lasts longer in a certain position, might produce more precipitation at a location nearby, it makes nonetheless sense to regard it as more than one event. The same holds true for the climate signal in Sect. 7 (Fig. 16c, d). For the composite differences two different core pressure ranges were distinguished: below 990 hPa, typical of well developed large-scale lows over the North Atlantic and 990–1010 hPa, typical of rather shallow lows over the Mediterranean or at southern midlatitudes (cf. Ulbrich et al, 1999). Figure 11 shows the composite differences for the frequency of deep cyclones. It becomes clear that the ATL region is strongly influenced by cyclones of the North Atlantic storm track. The southward shift of their tracks in high precipitation months agrees with the findings for baroclinicity and storm track activity. The two other

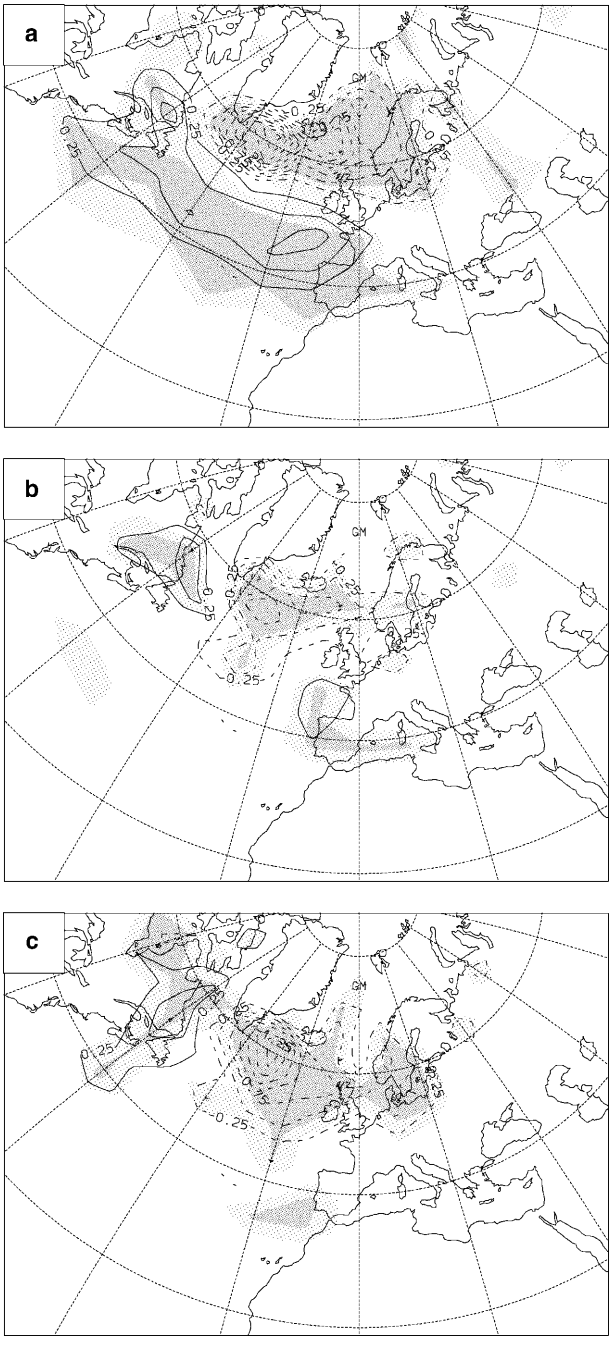

Fig. 11. Same as Fig. 8, but for frequency of cyclones with core pressures below 990 hPa. Contour interval is 0.25 cyclone days (1 cyclone day means that a cyclone core was identified in the respective 5° × 10° grid box during one day of the respective month)

regions reveal no significant dependency on this cyclone type apart from reduced activity over the northern North Atlantic for the SOA region. Nevertheless, all three regions show a strong influence of the activity of shallow local cyclones (Fig. 12). For the ATL region these cyclones are typically located at either side of the Iberian Peninsula with a slight maximum at the western side. Ulbrich et al (1999) found that for a given westerly humidity advection the occurrence of a local cyclone further enhances the amount of precipitation over Portugal, presumably due to the large-scale ascent at its fronts. SOA region precipitation is mainly connected to cyclones close to the southwestern tip of the Iberian Peninsula. Cyclones over the Western Mediterranean, that often enter from the Iberian Peninsula or through the Strait of Gibraltar (Trigo and Davies, 1999), are clearly most important for rainfall in the MED region. For all three regions, the local cyclones do not seem to be connected to the large-scale baroclinicity fields (see Fig. 8) but rather to the occurrence of upper level troughs (Fig. 9), whose position (black dots in Fig. 12) corresponds quite well to the signal in local cyclone activity, in particular for the MED and the SOA region, where no strong influence of deep Atlantic cyclones could be diagnosed. The fact that the maximum in cyclone frequency for MED (Fig. 12b) is located slightly east of the minimum in 500 hPa geopotential height (Fig. 9) might be at least partly due to the counting of cyclones in 5° lat × 10° lon boxes. The nearly vertical axis between the maxima of the upper- and low-level fields indicate the frequent occurrence of cut-off lows. Even though the region south of the Atlas is a region of frequent cyclogenesis (Trigo and Davies, 1999) the composite study yield no distinct anomaly over this area indicating little influence of the so called Sharav cyclones on Moroccan precipitation.

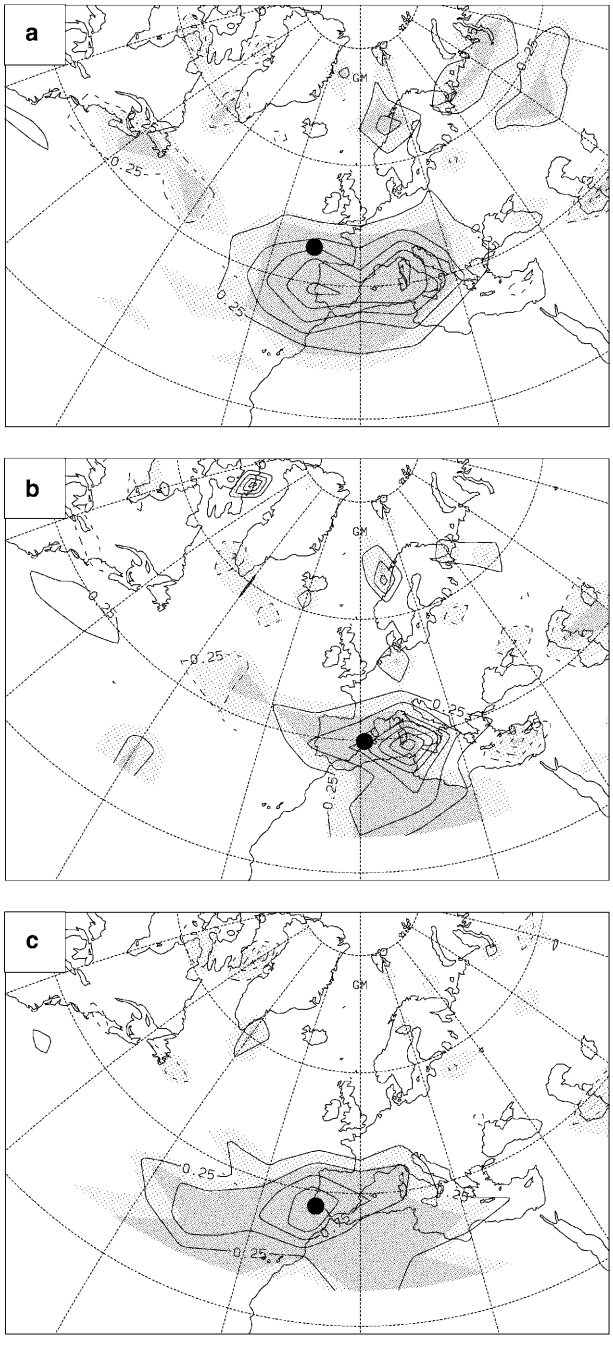

Fig. 12. Same as Fig. 11, but for frequency of cyclones with core pressures between 990 hPa and 1010 hPa. Contour interval is 0.25 cyclone days. Black dots represent the minima of geopotential height at 500 hPa from Fig. 9

An important factor for precipitation generation is, of course, the supply of moisture. Figure 13 shows the composite differences (wet minus dry) for the two components of the 850 hPa humidity advection (as vectors) and the correlations between its absolute value and the precipitation indices (as isolines). The influence of the local cyclones (Fig. 12) is clearly reflected in the humidity transport fields. Especially for the MED and the SOA region the location of the strongest positive anomalies in shallow cyclone frequency (black dots in Fig. 13) and the centres of the humidity advection vortices are nearly identical underlining the importance of these features for precipitation in both regions. For the ATL region, where also deep cyclones are of importance, the centre of the vortex is located northwest of the

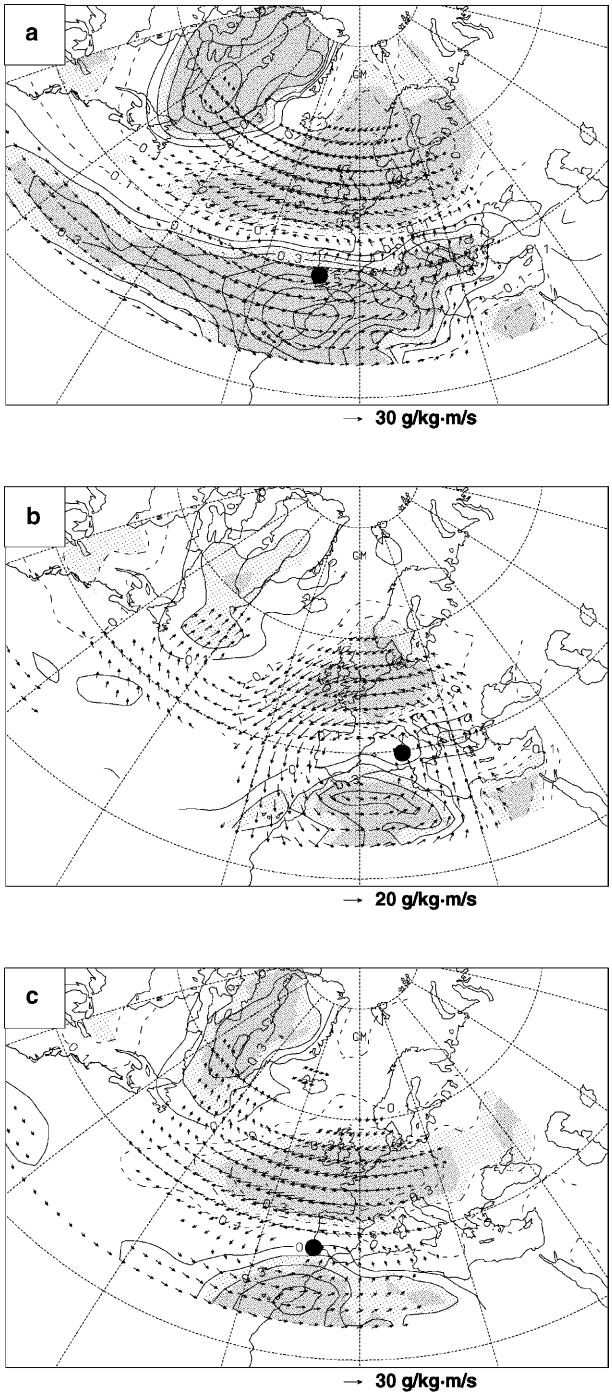

Fig. 13. Composite differences (wet minus dry) for humidity advection at 850 hPa (vectors) and correlation of monthly precipitation indices with the absolute value of humidity advection at the respective grid point (isolines) for winter (DJF). Only vectors representing more than a value of 7 g/kg · m/s are plotted. Contour interval for the correlation is 0.1. Black dots represent the maxima of the frequency of cyclones with core pressures between 990 hPa and 1010 hPa from Fig. 12. Light and dark shading indicates statistical significance at the 95% and 99% level, respectively; **a** ATL, **b** MED, and **c** SOA region (for definitions of the regions see Fig. 1)

Iberian Peninsula. The MED region shows correlations of up to 0.5 directly over the area of interest, whereas the other regions have maximum correlations just over the Atlantic coast (up to 0.75 ATL region and 0.55 SOA region). The position of the maximum for the SOA region just east of the Canary Islands reveals the importance of moisture input from the Atlantic ocean along the southern flank of the High Atlas into the area of interest. For the ATL region the high correlations with moisture transports from the Atlantic explains the connection between precipitation and westerly circulation types found in Sect. 5. The fact that there is a band of significant positive correlations nearly over the whole Atlantic underlines the dependency of this areas' precipitation on the behavior of the activity of the entire North Atlantic storm track.

7. Climate change projection

Precipitation is a quantity that is not always well reproduced in GCMs, especially where local or orographic influences are dominating. It has been further shown that GCM precipitation changes are not always in agreement with large-scale circulation changes (von Storch et al, 1993). It is therefore an important question, to what extent predicted changes in precipitation due to increased greenhouse gas forcing can be assigned to changes in large-scale baroclinic or synoptic activity, that is generally simulated with greater reliability.

To assess the impact of climate change on Moroccan winter precipitation, we consider data from a 240 year transient greenhouse gas only experiment conducted with the coupled general circulation model (GCM) ECHAM4/OPYC3. The atmospheric model ECHAM4 (European Centre model HAMburg version) has a spectral resolution of T42 (roughly $2.8^\circ \times 2.8^\circ$) and 19 irregularly spaced vertical levels. For a detailed description see Roeckner et al (1992 and 1996a). The oceanic component is the fully dynamical 11-layer OPYC (Ocean and isoPYCnal coordinates) model (Oberhuber, 1993). The model components are coupled quasi-synchronously and exchange information about surface fluxes of momentum, heat, freshwater etc. and sea surface temperature and sea ice variables once a day. More details on the coupling technique

and on the performance of the model can be found in Roeckner et al (1996b), and Bacher et al (1998). The anthropogenic greenhouse gas forcing is prescribed using observed data between 1860 and 1990, and the IS92a scenario (IPCC, 1992) thereafter, that assumes a further increase in CO_2 concentrations by ca. 500 ppm until 2100. Individual greenhouse gases are treated separately with regard to their contribution to the net radiative forcing. Effects from sulphate aerosols and tropospheric ozone are not taken into account. The model simulation is initialized with present-day values rather than pre-industrial ones. This causes a warm bias in the initial state of the scenario run which is maintained throughout the simulation and is regarded to have negligible impact on climatic trends. Further details on this simulation are given in Roeckner et al (1998).

Knippertz et al (2000) investigated the changes in synoptic and baroclinic activity over the North Atlantic and Europe comparing 50 winter (DJF) means from the beginning (control period) and the end (scenario period) of the 240 year transient integration, that differ by an additional forcing of about $6\,W/m^2$ due to the increased concentrations of CO_2 and other greenhouse gases. During the control period, the model reproduces most of the features found in NCEP and ECMWF re-analysis data well. Some problems, however, can be identified: In the mean wintertime SLP climatology the Azores High is shifted to the northeast and reaches a maximum pressure about 5 hPa higher than in the NCEP re-analysis. Consequently, the number of anticyclonic and easterly CWTs is too high and the number of cyclonic and westerly CWTs is too low in the model (see Table 3). The upper-tropospheric baroclinicity field is shifted to the east as well. With regard to the frequency of deep cyclones a comparison with climatologies shows a good agreement in structure, but an underestimation of the number of cyclones with core pressures less than 970 hPa by more than 50%, presumably due to the higher resolution of the re-analysis data with more distinct local extremes and sharper pressure gradients. Mediterranean cyclones are relatively small in scale and generally quite shallow and are not well represented in a coarse resolution model like the ECHAM4, even though a local maximum is visible over the Mediterranean in the model. 500 hPa storm track activity is underestimated by about 10% with regard to observed values. Note, that parts of this discrepancy might result from decadal variability or data problems in the re-analysis.

As mentioned above, coarse resolution GCMs like the ECHAM4 are unable to simulate regional features of Moroccan precipitation like the maxima over the Rif or the Atlas mountains. In addition, winter precipitation is generally a bit too low over Morocco during the control period of the ECHAM4/OPYC3 simulation compared to station measurements (not shown), which is presumably due to the too high pressure over the Iberian Peninsula that the model produces. With increasing greenhouse gas concentrations the ECHAM4/OPYC3 simulates decreasing precipitation particularly over the west coast of the Iberian Peninsula (Fig. 14). In Morocco changes of 35 mm in the north and about 10 mm in the south are reached (corresponding to relative changes of -15% to -25%). These changes shall be evaluated in the following with respect to their consistency with projected changes in the large-scale atmospheric circulation and synoptic activity (taken from Knippertz et al, 2000) using the relation identified in Sections 4 to 6. As the model's low-level fields (e.g., mean sea-level pressure) are little realistic over Greenland, this area is left blank in all following figures showing low-level quantities.

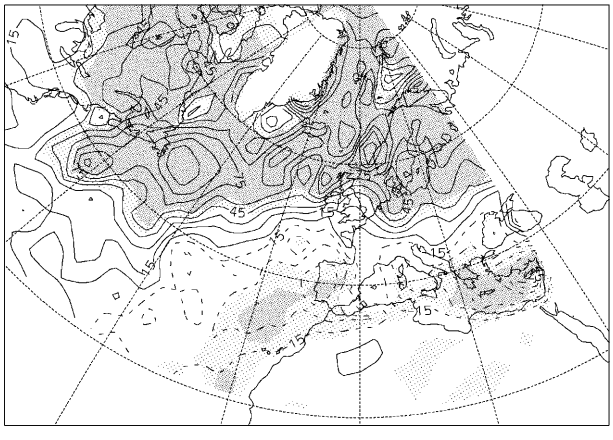

Fig. 14. Climate signal for winter (DJF) precipitation from the ECHAM4/OPYC3 transient greenhouse gas simulation. Differences are calculated between two 50 year periods from the beginning and the end of the 240 year run. Contour interval is 15 mm per season (DJF). Light and dark shading indicates statistical significance at the 95% and 99% level, respectively

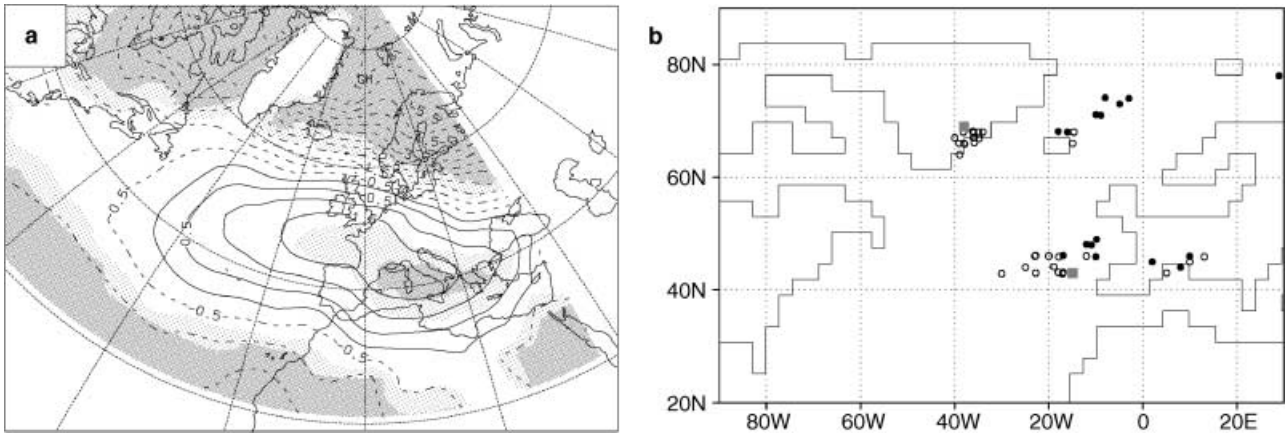

Fig. 15a. Same as Fig. 14, but for sea-level pressure. Contour interval is 0.5 hPa. **b** Locations of NAO centres as computed from EOF analyses of SLP fields. The mean position in the entire control run (using winter means) are marked by grey squares, those of consecutive decades in the scenario run (using all individual months) are marked by open circles before year 2020 and by black dots thereafter (taken from Ulbrich and Christoph, 1999)

The ECHAM4/OPYC3 simulates a strong and statistically significant decrease (up to 6 hPa) of SLP north of about 58° N from Eastern Europe to Eastern North America (Fig. 15a) and weakly enhanced pressure over Southern and Western Europe. The rising pressure over Southwestern Europe coincides with the eastward shift of the southern centre of the NAO in the course of the simulation (Fig. 15b, taken from Ulbrich and Christoph, 1999). During relatively northeasterly positions of the Azores High in winter Morocco is located at the southern flank of the anticyclone having mostly easterly weather situations. The changes in the mean SLP field has therefore a distinct influence on the frequency of circulation types (Table 3). While the frequency of westerly (SW, W and NW) and northerly circulation types is substantially reduced, easterly and in particular southeasterly situations get much more frequent with increasing greenhouse gas concentrations. The northward shift of the southern NAO pole reduces the probability of the anticyclonic centre to be over Morocco by about 5%. According to the findings in Sections 4 and 5 these changes should have a negative influence on precipitation for the ATL and the MED region, where westerly and northerly circulation types were found to be of major importance. For the SOA region the situation is not so clear. Negative influences due to the decreasing frequency of the most important CWTs (cyc, SW) might be compensated by the distinct plus in easterly and southeasterly situations, which were found to have a weak, but positive influence on precipitation (see Sect. 5). It is questionable, however, if enough moisture from the Atlantic is transported into the region, when less westerly situations occur under changed large-scale conditions.

The changes in baroclinic and synoptic activity shall be investigated looking at the Eady parameter, storm track intensity (for definition of both parameters see Section 6) and cyclone frequency again. With increased greenhouse gas concentration changes in the mean temperature induce a northward shift of the zone of high baroclinicity in the upper troposphere over the North Atlantic (Fig. 16a). In the lower troposphere a reduction in the meridional temperature gradient and the land-sea contrasts leads to decreased or unchanged baroclinicity over most of the North Atlantic and Europe (not shown). The climate signal in storm track activity (Fig. 16b) shows a strong increase (+ 15%) over the eastern North Atlantic and Europe and region of decreased storm track activity south of 45° N over the Atlantic, the Mediterranean and North Africa with a minimum of about – 3 gpm over the Central North Atlantic. For this simulation cyclone core positions and pressures were identified by means of an automatic identification routine (Haak and Ulbrich, 1996) based on twice daily (00 and 12 UTC) 1000 hPa geopotential height data, that gives similar results than the scheme used in Sect. 6. Cyclone cores are counted in 5° lat × 10° lon grid boxes for the same core pressure ranges as in Sect. 6. Again no tracking was done. In correspondence

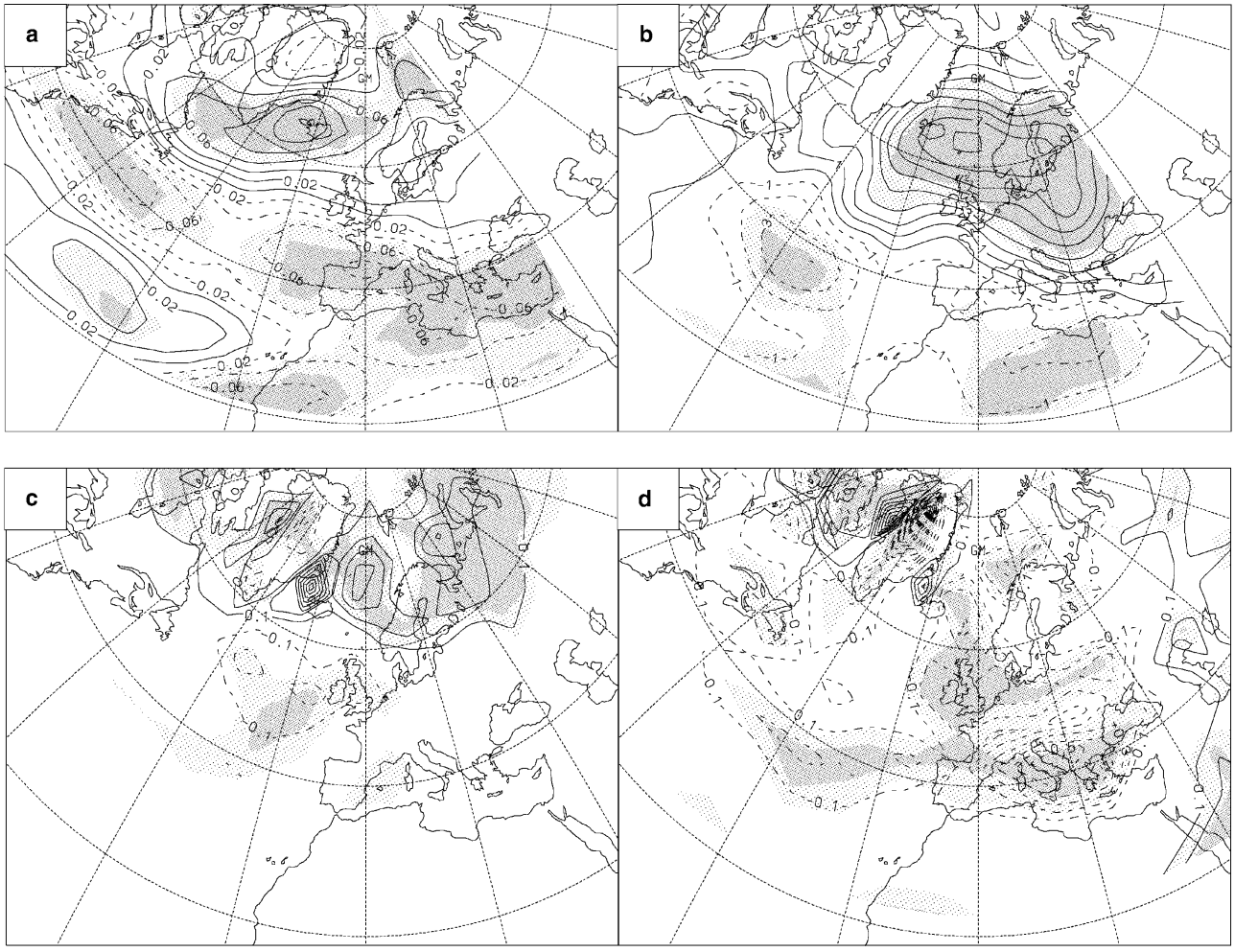

Fig. 16. Same as Fig. 14, but for synoptic activity: **a** upper-tropospheric baroclinicity (measured by the maximum Eady growth rate for the 300 hPa to 500 hPa layer, see text for definition), **b** storm track activity (measured by the 2.5 to 8 day bandpass filtered 500 hPa geopotential height standard deviation, see Christoph et al, 1995), frequency of cyclones with core pressures, **c** below 990 hPa, and **d** between 990 hPa and 1010 hPa. Contour interval is 0.02 day^{-1} in (**a**), 1 gpm in (**b**) and 0.1 cyclone days (1 cyclone day means that a cyclone core was identified in the respective $5^\circ \times 10^\circ$ grid box during one day of the respective month) in (**c**) and (**d**)

with the upper-tropospheric baroclinicity and the storm track climate signal the frequency of deep cyclones (core pressure <990 hPa, Fig. 16c) undergoes a pronounced northward shift over the eastern North Atlantic. This shift of the entire North Atlantic storm track system is the reversal of what was found to be characteristic of high precipitation months for the ATL region in Section 6. In accordance to what was found with respect to changes in the NAO and the SLP distribution, the predicted decrease in precipitation can be easily understood in terms of the changes in large-scale synoptic activity for the ATL region. For the other two regions, however, local cyclone activity was found to be more important for precipitation generation. Here (for cyclone frequency in the core pressure range from 990 to 1010 hPa, Fig. 16d) an over-all decrease is identified, particularly for the Mediterranean (-30% to -40%), but also for the Atlantic around 40° N. With respect to the results from Section 6, weakening activity over the Western Mediterranean suggests decreasing precipitation for the MED region. The frequency of cyclones southwest of the Iberian Peninsula is nearly unchanged, so that no clear implications for the precipitation in the SOA region arise from these results.

8. Summary and conclusions

In this study, the observed relation between Moroccan winter (DJF) precipitation and the

large-scale circulation and synoptic activity and possible future changes were investigated on a monthly basis. As the investigations have been carried out for a number of meteorological quantities, a rather complete picture of the large-scale conditions that are favourable for precipitation generation is achieved.

Three regions have been distinguished, for which precipitation indices were calculated: the *Atlantic region* (Northwestern Morocco and the Atlantic coast, ATL), the *Mediterranean region* (Northwestern Algeria and Northeastern Morocco, MED) and the *Atlas region* (Morocco and Algeria south of the Atlas, SOA). Time series of annual precipitation indices for these regions reveal very dry 1980s and 1990s in MED, a dry period from the late 1970s to the early 1990s in ATL, but a relatively wet period 1985–1998 in SOA. In summary, the main characteristics of the large-scale circulation in high precipitation months are the following:

ATL: a southerly shift of (a) the tracks of North Atlantic cyclones, (b) upper tropospheric baroclinicity and (c) storm track activity over the entire North Atlantic, (d) locally enhanced cyclone activity over the Atlantic and the Mediterranean, (e) low 500 hPa geopotential height north west of the Iberian Peninsula, (f) strongly enhanced westerly humidity advection, (g) an increased frequency of westerly and northwesterly weather types, and (h) a weak or westward displaced southern NAO pole.

MED: (a) low 500 hPa geopotential height, and (b) a highly significant enhanced frequency of cyclones over the Western Mediterranean, (c) locally enhanced storm track activity, (d) enhanced northwesterly humidity advection, and (e) a high number of northerly circulation weather types.

SOA: (a) low geopotential height, and (b) the occurrence of cyclones southwest of the Iberian Peninsula, (c) above normal storm track activity over the Canary Islands, (d) enhanced humidity transports from the Atlantic near the Canary Islands along the southern flank of the Atlas, and (e) a high number of cyclonic, southwesterly and southerly circulation weather types.

Results for the ATL region reveal clear dependencies on the synoptic activity over the Atlantic. Many results for this region, like the southward shift of the storm track in high precipitation months, the importance of local cyclones and westerly humidity advection as well as the role of the NAO, agree with studies for the Iberian Peninsula (Zorita et al, 1992; Rodó et al, 1997; Zhang et al, 1997; Ulbrich et al, 1999; Trigo and DaCamara, 2000). Correlations with SLP, however, show that the NAO influence is to a considerable extent a regional rather than a teleconnection effect ($r = -0.81$ at Gibraltar). A correlation with the ''classical'' NAO index based on the pressure over the Azores and Iceland (cf. Lamb and Peppler, 1987; Lamb et al, 1997; Ward et al, 1999) is substantially lower ($r = -0.49$). In contrast to ATL, both the MED and the SOA region show no distinct dependency on the North Atlantic storm track and the NAO. Nevertheless, the strong link to the occurrence of cyclones over the Western Mediterranean provides a good understanding of precipitation variability in the MED region. Mechanisms for precipitation generation in the SOA region, however, appear to be more complex. It is clear that the Atlantic is the main moisture source for this region and that a transport along the southern flank of the Atlas due to the air flow south of local cyclones is a crucial point. In addition precipitation appears to be linked to the occurrence of upper tropospheric troughs or cut-off lows, which reduce the static stability over the region and lead to dynamical uplift downstream of the trough axis. The relation to southerly weather types suggests that the orography might play an important role, too. Orographic lifting at the southern slope of the Atlas that generates convective or even large-scale precipitating clouds, if enough moisture is available in lower levels, could be one possible mechanism for precipitation generation. In the case of convection, stability would be a limiting factor. The relative importance of this process, however, can hardly be determined from monthly data. It is also an open question, whether large-scale precipitation areas connected to fronts of local cyclones reach the SOA region or if rather local generation is of greater relative importance. Presumably only investigations based on daily data, that enable to study single events, can give answers to these questions.

The second step of this study consisted in viewing the mechanisms for precipitation in Morocco under the light of the results from a

climate simulation with the fully coupled GCM ECHAM4/OPYC3 for increasing greenhouse gas concentrations. The predicted changes that appear to be relevant for Moroccan precipitation are the following: (a) a northward shift of the North Atlantic upper tropospheric baroclinicity, deep cyclone tracks and storm track activity, (b) a decrease in the number of shallow cyclones over the Mediterranean and parts of the Atlantic, (c) an east to northeastward shift of the southern NAO pole leading to (d) less westerly and more easterly weather situations over Morocco. This climate signal can be interpreted with respect to precipitation in the three regions considered in order to evaluate the model predicted precipitation changes. The northward shift of synoptic activity over the North Atlantic and the eastward shift of the Azores High explain the model predicted decrease in precipitation (Fig. 14) for ATL quite well. As shown in Sect. 7, however, the model reveals certain problems in reproducing the climatological position of the Azores High, which weakens the reliability of this result. Nevertheless, the ECHAM4 is a physically based model that gives an over-all good representation of the world's large-scale circulation. Therefore the model's internal response to an increased GHG forcing regarding the large-scale circulation and synoptic activity, is in fact meaningful. In addition to that, other GCMs equally simulate a northward shift of the storm track over the North Atlantic with increasing greenhouse gas concentrations (e.g., Hall et al, 1994; König et al, 1993). It would be nonetheless desirable to conduct similar investigations with the output from other climate simulations to further corroborate our results. For MED the decreased number of cyclones over the Western Mediterranean and the reduced frequency of northerly weather situations make the simulated decrease in precipitation comprehensible from the point of view of the large-scale circulation changes. This results should, however, also be regarded with some caution, since Mediterranean cyclones are not particularly well simulated in coarse resolution climate models. According to Trigo and Davies (1999) a high resolution (ca. 1.125°) is needed to identify subsynoptic-scale Mediterranean lows in analysis data. It should be mentioned, however, that a distinct reduction of precipitation in this region has already occurred during the last two decades (see Fig. 4). In SOA precipitation is mainly influenced by local processes (shallow cyclones, orography, presumably local convection etc.). This makes a climate prediction with a coarse resolution climate model extremely difficult. The fact that southerly and southeasterly weather situations have a positive influence on precipitation in this region (see Sect. 5) indicates the importance of orographic lifting. Since the Atlas mountains have only about one fourth of their actual height in the model, this influence factor is quite badly represented in the simulation. A regional downscaling of GCM results might shed some light into this problem, but a statistical method as used by von Storch et al (1993) requires a strong link between precipitation and the large-scale SLP field, which is only true for the ATL region and can not explain any physical mechanisms. Dynamical downscaling with a meso-scale meteorological model, however, can only be used for limited period studies, in particular because of the high need of computer capacity, but even these might help to understand possible changes. The use of a statistical–dynamical downscaling scheme (e.g., Fuentes and Heimann, 2000) that can be applied to long-term studies may help to overcome some of the problems of the pure statistical or pure dynamical methods.

Two main tasks remain to solve some of the open questions: the physical concepts with respect to the reasons for precipitation variability in Morocco that evolved from this study are to be extended and refined using more event-based investigations with daily precipitation data or studies with a meso-scale meteorological model. Furthermore, data from additional stations, especially in the mountains and south of the Atlas, where only little data has been available for this study, would certainly help to better understand more local influence factors (orography, local convection etc.).

Acknowledgements

This work is part of the IMPETUS (''An Integrated Approach to the Efficient Management of Scarce Water Resources in West Africa'') project and was supported by the Federal German Ministry of Education and Research (BMBF) under grant no. 07 GWK 02 and by the Ministry of Education, Science and Research (MSWF) of the federal state of Northrhine-Westfalia under grant no. 514-21200200. We

thank R. S. Vose from the Office of Climatology of the Arizona State University and N. Filali Boubrahmi from the Direction de la Météorologie Nationale for providing the precipitation data. The authors would like to thank the two anonymous reviewers whose comments and suggestions contributed to improve the manuscript.

References

Bacher A, Oberhuber MJ, Roeckner E (1998) ENSO dynamics and seasonal cycle in the tropical Pacific as simulated by the ECHAM4/OPYC3 coupled general circulation model. Clim Dyn 14: 431–450

Beniston M, Fox DG (1996) Impacts of climate change on mountain regions. In: Climate change 1995: Impacts, adaptations and mitigation of climate change: Scientific-technical analyses, chap. 5. Watson RT, Zinyowera MC, Moss RH, Dokken DJ (eds). Cambridge: Cambridge University Press

Bullock P, Le Houérou H (1996) Land degradation and desertification. In: Climate change 1995: Impacts, adaptations and mitigation of climate change: Scientific-technical analyses, chap. 4. Watson RT, Zinyowera MC, Moss RH, Dokken DJ (eds). Cambridge: Cambridge University Press

Charney JG (1947) The dynamics of long waves in a baroclinic westerly current. J Meteor 4: 135–162

Chbouki N, Stockton CW, Myers D (1995) Spatio-temporal patterns of drought in Morocco. Int J Climatol 15: 187–205

Christoph M, Ulbrich U, Haak U (1995) Faster determination of the intraseasonal variability of storm tracks using Murakami's recursive filter. Mon Wea Rev 122: 578–581

Eady ET (1949) Long waves and cyclone waves. Tellus 1: 33–52

El Hamly M, Sebbari R, Lamb PJ, Ward MN, Portis DH (1998) Towards the seasonal prediction of Moroccan precipitation and its implication for water resources management. Water resources variability in Africa during the 20th century (Proc. of the Abidjan '98 Conf. held at Abidjan, Côte d'Ivoire, November, 1998). IAHS Publ. No. 252, 79–87

Fuentes U, Heimann D (2000) An improved statistical–dynamical downscaling scheme and its application to the Alpine precipitation climatology. Theor Appl Climatol 65: 119–135

García Herrera R, Gallego Puyol D, Hernández Martín E, Gimeno Presa L, Ribera Rodríguez P (2001) Influence of the North Atlantic Oscillation on the precipitation in the Canary Islands. J Clim 14: 3889–3903

Gleick PH (1992) Effects of climate change on shared fresh water resources. In: Confronting climate change: Risks, implications and responses, chap. 9. Mintzer IM (ed). Cambridge: Cambridge University Press

Griffiths JF (1972) The Mediterranean zone. In: World survey of climatology, Vol. 10: Climates of Africa, chap. 2, Landsberg HE (ed). Amsterdam London New York: Elsevier

Haak U, Ulbrich U (1996) Verification of an objective cyclone climatology for the North Atlantic. Meteorol Z 5: 24–30

Hall NMJ, Hoskins BJ, Valdes PJ, Senior CA (1994) Storm tracks in a high-resolution GCM with doubled carbon dioxide. Q J Roy Meteor Soc 120: 1209–1230

Hoskins BJ, Valdes PJ (1990) On the existence of storm-tracks. J Atmos Sci 47: 1854–1864

Hulme M (1992) Rainfall changes in Africa: 1931–1969 to 1961–1990. Int J Climatol 12: 685–699

Hurrell JW, van Loon H (1997) Decadal variations in climate associated with the North Atlantic oscillation. Clim Change 36: 301–326

IPCC (1992) Climate change 1992: The supplementary report to the IPCC scientific assessment. Cambridge: Cambridge University Press

Jones PD, Hulme M, Briffa KR (1993) A comparison of Lamb weather types with an objective classification scheme. Int J Climatol 13: 655–663

Jones PD, Jónsson T, Wheeler D (1997) Extension to the North Atlantic Oscillation using early instrumental pressure observations from Gibraltar and South-West Iceland. Int J Climatol 17: 1433–1450

Kalnay E, Kanamitsu M, Kistler R, Collins W, Deaven D, Gandin L, Iredell M, Saha S, White G, Woollen J, Zhu Y, Leetmaa A, Reynolds R, Chelliah M, Ebisuzaki W, Higgins W, Janowiak J, Mo KC, Ropelewski C, Wang J, Jenne R, Joseph D (1996) The NCEP/NCAR 40-year reanalysis project. Bull Am Met Soc 77: 437–471

Katz RW, Glantz MH (1986) Anatomy of a rainfall index. Mon Wea Rev 114: 764–771

Knippertz P, Ulbrich U, Speth P (2000) Changing cyclones and surface wind speeds over the North Atlantic and Europe in a transient GHG experiment. Clim Res 15: 109–122

König W, Sausen R, Sielmann F (1993) Objective identification of cyclones in GCM simulations. J Clim 6: 2217–2231

Lamb PJ, Peppler RA (1987) North Atlantic Oscillation: concept and application. Bull Am Met Soc 68: 1218–1225

Lamb PJ, El Hamly M, Portis DH (1997) North-Atlantic Oscillation. Géo Observateur 7: 103–113

Lindzen RS, Farrel B (1980) A simple approximate result for the maximum growth rate of baroclinic instabilities. J Atmos Sci 37: 1648–1654

Murray RJ, Simmonds I (1991) A numerical scheme for tracking cyclone centres from digital data. Part I: Development and operation of the scheme. Aust Met Mag 39: 155–166

Nicholson SE (1986) The spatial coherence of African rainfall anomalies: Interhemispheric teleconnections. J Clim Appl Meteorol 25: 1365–1381

Nicholson SE, Kim J (1997) The relationship of the El Niño-Southern Oscillation to African rainfall. Int J Climatol 17: 117–135

Oberhuber JM (1993) Simulation of the Atlantic circulation with a coupled sea ice-mixed layer – isopycnal general circulation model. Part I: Model description. J Phys Oceanogr 22: 808–829

Parish R, Funnell DC (1999) Climate change in mountain regions: Some possible consequences in the Moroccan High Atlas. Global Environ Chang 9: 45–58

Portis DH, Walsh JE, El Hamly M, Lamb PJ (2001) Seasonality of the North Atlantic Oscillation. J Clim 14: 2069–2078

Rasmusson EM, Carpenter TH (1983) The relationship between eastern equatorial Pacific sea surface temperatures and rainfall over India and Sri Lanka. Mon Wea Rev 11: 517–528

Rodó X, Baert E, Comin FA (1997) Variations in seasonal rainfall in Southern Europe during the present century: relationship with the North Atlantic Oscillation and the El Niño-Southern Oscillation. Clim Dyn 13: 275–284

Roeckner E, Arpe K, Bengtsson L, Dümenil L, Esch M, Kirk E, Lunkeit F, Ponater M, Rockel B, Sausen R, Schlese U, Schubert S, Windelband M (1992) Simulation of present-day climate with the ECHAM model: Impact of model physics and resolution. Report No. 93, Max-Planck-Institut für Meteorologie, Hamburg

Roeckner E, Arpe K, Bengtsson L, Christoph M, Claussen M, Dümenil L, Esch M, Giorgetta M, Schlese U, Schulzweida U (1996a) The atmospheric general circulation model ECHAM4: Model description and simulation of present-day climate. Report No. 218, Max-Planck-Institut für Meteorologie, Hamburg

Roeckner E, Oberhuber JM, Bacher A, Christoph M, Kirchner I (1996b) ENSO variability and atmospheric response in a global coupled atmosphere-ocean GCM. Clim Dyn 12: 737–754

Roeckner E, Bengtsson L, Feichter J, Lelieveld J, Rhode H (1998) Transient climate change simulations with a coupled atmosphere-ocean GCM including the tropospheric sulphur cycle. Report No. 266, Max-Planck-Institut für Meteorologie, Hamburg

Rogers JC (1984) The association between the North Atlantic Oscillation and the Southern Oscillation in the northern hemisphere. Mon Wea Rev 112: 1999–2015

Stockton CW, Glueck MF (1999) Long-term variability of the North Atlantic Oscillation (NAO). Proc. of the 10th Symp. on global change studies. Amer Meteorol Soc, 10–15 January, 1999, Dallas, Texas

Taubenheim J (1969) Statistische Auswertung geophysikalischer und meteorologischer Daten. Leipzig: Akademische Verlagsgesellschaft

Trigo IF, Davies TD (1999) Objective climatology of cyclones in the Mediterranean region. J Clim 12: 1685–1696

Trigo RM, DaCamara CC (2000) Circulation weather types and their influence on the precipitation regime in Portugal. Int J Climatol 20: 1559–1581

Ulbrich U, Christoph M (1999) A shift of the NAO and increasing stormtrack activity over Europe due to anthropogenic greenhouse gas forcing. Clim Dyn 15: 551–559

Ulbrich U, Christoph M, Pinto JG, Corte-Real J (1999) Dependence of winter precipitation over Portugal on NAO and baroclinic wave activity. Int J Climatol 19: 379–390

von Storch H, Zorita E, Cubasch U (1993) Downscaling of global climate change estimates to regional scales: An application to Iberian rainfall in wintertime. J Clim 6: 1161–1171

Vose RS, Schmoyer RL, Steurer PM, Peterson TC, Heim R, Karl TR, Eischeid JK (1992) The Global Historical Climatology Network: Long-term monthly temperature, precipitation, sea level pressure, and station pressure data. NDP-041. Carbon Dioxide Information Analysis Center, Oak Ridge National Laboratory, Oak Ridge, Tennessee

Ward MN, Lamb PJ, Portis DH, El Hamly M, Sebbari R (1999) Climate variability in Northern Africa: Understanding droughts in the Sahel and the Maghreb. In: Beyond El Niño – Decadal and interdecadal climate variability, chap. 6. Navarra A (ed). Berlin Heidelberg New York: Springer

Youbi L (1990) Hydrologie du bassin du Dades. Available from: Ministère de l'Agriculture et de la Reforme Agraire, Office Régional de Mise en Valeur Agricole de Ouarzazate (ORMVAO), Avenue Mohamed V, B.P. 29–95, Ouarzazate, Morocco

Zhang X, Wang X, Corte-Real J (1997) On the relationship between daily circulation patterns and precipitation in Portugal. J Geophys Res 102: 13495–13507

Zorita E, Viacheslav K, von Storch H (1992) The atmospheric circulation and sea surface temperature in the North Atlantic area in winter: Their interaction and relevance for Iberian precipitation. J Clim 5: 1097–1108

Authors' address: Peter Knippertz (E-mail: knippertz@meteo.uni-koeln.de), Dr. Michael Christoph (E-mail: christoph@meteo.uni-koeln.de) and Prof. Dr. Peter Speth (E-mail: speth@meteo.uni-koeln.de), Institut für Geophysik und Meteorologie, Universität zu Köln, Kerpener Str. 13, D-50923 Köln, Germany